Liquid Crystals
Publication details, including instructions for authors and subscription information:
http://www.informaworld.com/smpp/title~content=t713926090

The vitreous gel: a composite structured network engineered by Nature

Alberto Ciferri[a]; Alessandro Magnasco[b]
[a] Chemistry Department, Duke University, Durham, N.C. 27708-0354, USA [b] Ophthalmology Department, Villa Scassi Hospital, 16100 Genoa, Italy

To cite this Article Ciferri, Alberto and Magnasco, Alessandro(2007) 'The vitreous gel: a composite structured network engineered by Nature', Liquid Crystals, 34: 2, 219 — 227
To link to this Article: DOI: 10.1080/02678290601137692
URL: http://dx.doi.org/10.1080/02678290601137692

Liquid Crystals, Vol. 34, No. 2, February 2007, 219–227

The vitreous gel: a composite structured network engineered by Nature

ALBERTO CIFERRI*† and ALESSANDRO MAGNASCO‡
†Chemistry Department, Duke University, Durham, N.C. 27708-0354, USA
‡Ophthalmology Department, Villa Scassi Hospital, 16100 Genoa, Italy

(*Received 8 August 2006; accepted 10 October 2006*)

The vitreous body of the eye is a gel composed primarily of water and an ordered distribution of collagen II fibrils reinforcing a hyaluroran network. Its age-induced alteration leads to serious eye pathologies. Notwithstanding extensive biochemical investigation, its assembling mechanism is poorly understood. In this paper we analyse the vitreous components in terms of general principles governing their supramolecular interaction, mesophase behaviour and collagen fibrillogenesis. This basic approach allows the selection of assembling patterns consistent with experimental data in the literature. The conclusions may provide new guidelines for advanced therapy and nanotechnological replacement engineering.

1. Introduction

The human vitreous body is a clear gel occupying about 80% of the volume of the eyeball within the posterior compartment of the eye, figure 1 (*a*). The vitreous is composed mainly of water (~98%) in equilibrium swelling with aqueous humour at the anterior hyaloid face between the lens and ciliary body. Main macromolecular components include the fibrillar type II collagen (~75% of total collagen) and glycosaminoglycans, notably hyaluronan and chondroitin sulphate. Minor components include other fibrillar and non-fibrillar collagenous and non-collagenous proteins, extracellular matrix proteins (opticin), highly basic proteins, and acidic glycoproteins. Biosynthesis occurs primarily at cells located in the non-pigmented ciliary epithelium [1].

The vitreous gel helps to maintain the transparency of the media and supports the structures within the eye. Its viscoelastic properties allow the eye to return to its normal shape following compression [2]. A peculiar structural feature of the vitreous gel, schematized in figure 1 (*a*), is an ordered distribution of collagen fibrils within a structurless viscoelastic network. The normal human vitreous gel contains fibrils that insert posteriorly into the macula vitreous cortex (a 100–300 μm layer of collagen fibrils oriented parallel to the retinal surface), and anteriorly into the vitreous base as illustrated in figure 1 (*a*). The large hyaluronic acid molecules fill the spaces between the fibrils, but a definite assembly mechanism for this composite, structured network is still unavailable [1, 3].

Progressive gel liquefaction, figures 1 (*b*) and 1 (*c*) is a normal aging event resulting, in combination with weakening of the vitreoretinal adhesion, in posterior vitreous detachment (PVD). In that clinical situation, the vitreous cortex is dissected from the inner limiting lamina of the posterior retina by fluid vitreous. Flashes of light are a common symptom of PVD and are due to pulling on the retina as the gel separates. If a retinal blood vessel is broken in the pulling, a vitreous haemorrhage can occur. If the gel is abnormally adherent to the retina, or the retina is weak in a certain area, a retinal tear can occur as the gel separates and pulls away. Once a retinal tear develops there is a significant risk of liquid vitreous going through the break and detaching the retina from the back wall of the eye.

The organization of the gel and its age-related degradation has been the subject of extensive investigation. The complex biochemistry and *in vivo* functioning of the vitreous gel has led to a variety of often contradicting models for the underlying fundamental processes. The basic results and current models were comprehensively reviewed by Bishop [1]. Here we attempt to analyse the structurization, and ensuing degradation, using current concepts of polymer compatibility and self-assembly, aiming at an interpretation of the mechanisms and strategies by which the complex multi-component structure of the vitreous gel might have been assembled by Nature. We compare the expectations from our analysis with experimental data

*Corresponding author. Email: cifjepa@chimica.unige.it

Liquid Crystals
ISSN 0267-8292 print/ISSN 1366-5855 online © 2007 Taylor & Francis
http://www.tandf.co.uk/journals
DOI: 10.1080/02678290601137692

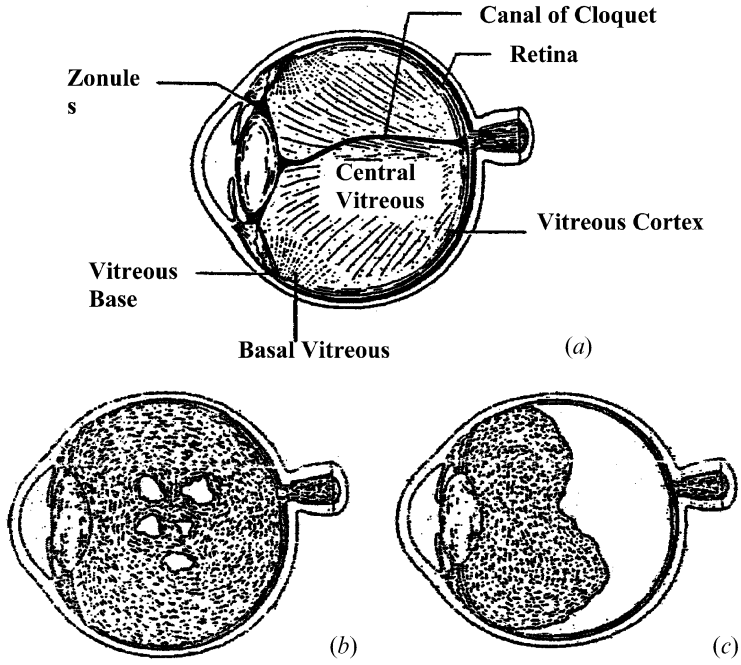

Figure 1. (*a*) The orientation of heterotypic collagen fibrils in the vitreous gel within a proteoglycan–hyaluronic acid matrix. The system is regarded here as a composite structured network. (*b*) Early liquefaction. (*c*) Posterior detachment. Taken from[1, 35].

reported in the literature for the main components defined above. The analysis offers definite supports to selected models under current discussion [1], and adds new insights on the genesis of the structured network, on the liquefaction process, and on the possibility of engineering artificial replacements.

In §2 we analyse data pertaining to the single components, concluding that their chemical and conformational incompatibility should have prevented any structurization. The ensuing §3 highlights how incompatibility was surmounted by chemically blocking selected components, and by a combination of attractive and repulsive supramolecular interactions resulting in the stabilization of the structured network.

2. Major single components

2.1. *Hyaluronic acid (HA)*

HA is a linear glucosaminoglycan (GAG) characterized by disaccharide repeating units linked by alternating β (1→3) and β (1→4) bonds (figure 2). The polymer is a polyanion due to the D-glucoronic acid residues and it is not covalently linked to protein carriers. HA is the major glycosaminoglycan component of human vitreous gel (65–400 $\mu g\,ml^{-1}$); its concentration is larger in the posterior vitreous gel and it increases with age [4, 5]. Molecular masses in the range 4×10^4–5.5×10^6, M_w/M_n 1.6–2.2, have been studied [6]; values between 2×10^6–4×10^6 ($DP \sim 7\,500$) were reported for human vitreous gel [5], and the value of 170 000 was reported for bovine vitreous gel [7].

Molecular dynamics simulation [8] allowed the construction of structures corresponding to the population of primary and secondary conformational minima for the β(1→3) and β(1→4) bonds. The most stable conformation is consistent with the left-hand helices deduced from X-ray fibre diffraction. The occurrence of other energy minima allows the expectation of conformational isomerism [8]. In fact, experimental and simulation determinations of persistence length (q) suggest a semi-rigid worm-like *local* conformation in solution (q, the average sum of the projection of chain bonds along a Cartesian axis where the first bond is located, is a measure of chain extension). H-bonds appear a significant cause of intramolecular rigidity and intermolecular interactions, possibly including tertiary structures [9].

Bathe *et al.* [10] recently reported $q \sim 7.1$ nm by coarse-grained simulation. Older data yielded an average $q \sim 6.0$ nm for ionic strength (i.s.) >0.1M [10]. Although larger than the persistence length of coiling polymers ($q < 1.0$ nm), the average value of q for HA reported in table 1 is close to the limit at which no liquid crystalline order is theoretically predicted [11]. The

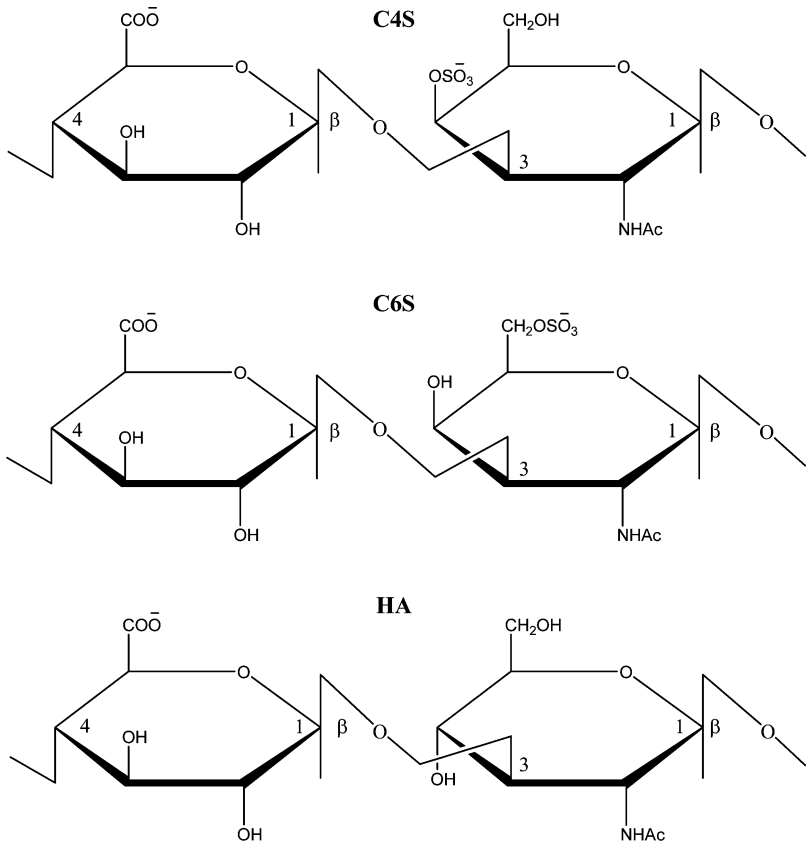

Figure 2. Disaccharide repeat units of C4S, C6S and HA.

global conformation of a worm-like chain having a contour length several multiples of q (as for HA of the vitreous gel) approaches the Gaussian coil limit [12]. Data in table 1 are close to the intrinsic persistent length (q_o) [13]. The electrostatic contribution q_e was also determined and reviewed [10]. The latter may attain values comparable to q_o at i.s. <0.1M. Such large contributions of electrostatic repulsion should not be expected under physiological pH and i.s. (~ 0.15M).

Studies of the non-Newtonian viscoelasticity of HA solutions are also relevant in assessing the structural and functional properties of the vitreous gel [14, 15]. Master curves revealed an excellent superimposition of storage and loss moduli over time–temperature–concentration–pH– i.s., interpreted as a breakdown of a labile H-bonded network followed by viscous flow. No evidence for covalent crosslinkages was also reported by Gribbon *et al.*, who investigated self and tracer-diffusion coefficients in concentrated HA solutions of varying pH and i.s. [16, 17].

Table 1. Near-intrinsic persistence lengths.

Component	q/nm	Reference
HA	6 ± 2	Average, cf. text
HA	7.1	[10]
C6S	7.1	[10]
C4S	9.6	[10]
Collagen helices	11.2	[26]
Aggregan	82.0	[20]

2.2. *Chondroitin sulphate (CS)*

CS is also a GAG based on the same sequence of disaccharide units linked by the alternating β (1→3) and β (1→4) bonds occurring in HA (figure 2). However, CS has a charge density larger than HA due to the strong acidic sulphate group on the 4- or 6-carbon of the *N*-acetyl-D-galactosamide residue. At variance with HA, CS is found in covalent associations to proteins (proteoglycans, cf. §3). Data in the present section refer to the CS component that can be separated from proteins [18, 19], studied by simulation [10], or by AFM [20] while attached to proteoglycans.

Sulphation occurs following biosynthesis, and details regarding its type (4-, or 6-), distribution, even the CS chain length vary with age, diseases and type of proteoglycan [20, 21]. In mammalian vitreous gel, both C4S and C6S occur [7]. The chain length appears to

be significantly smaller, e.g. 15–60 kD [1, 18], than indicated above for HA for human vitreous gel. Differences in the chain structure of C4S and C6S were indicated by hydrodynamic parameters and persistence lengths. From simulation studies [10], the q value for C4S is larger than for C6S (table 1), while the latter coincides with the value reported for HA. The local conformation of CS therefore exhibits a rigidity comparable to, or slightly larger than, HA. However, due to its greater chain length, the latter has a larger global flexibility and is better suited to contribute to the viscoelastic features of the vitreous gel.

2.3. *Collagen*

A number of related proteins are described as collagen, and their chemical/structural variations reflect different functional roles as extracellular matrix components. A fibrillar form (collagen II) and a non-fibrillar form (collagen IX) occur in the vitreous gel: a total concentration of $65\,\mu g\,ml^{-1}$ was reported for bovine vitreous gel [7]. Three α-chains, not necessarily with the same amino acid composition, associate in the typical tertiary structure of a triple-helix having a pitch of 10.4 nm, length $L\sim300$ nm, diameter $d\sim1.4$ nm [22]. As discussed by Fertala *et al.*, collagen II (α_1 $(II)_3$), based on three identical α_1 chains with short terminal telopeptide regions, has remarkable similarities with heterotrimer collagen I ($\alpha_1(I)_2\alpha_2I$) [23] and, indeed, a persistence length $q\sim11.2$ nm for both collagen I and collagen II was recently reported using optical tweezers under physiological conditions [24]. The non-fibrillar collagen IX has interrupted triple-helices forming a sequence of collagenous (COL1, COL2, COL3) and non-collagenous (NC1, NC2, NC3) blocks [1]. It can establish covalent links with collagen II and with CS chains (cf. §3).

The isoelectric pH of triple-helical collagen I solubilized from rat tail tendons is ~7.2; its weak polyelectrolyte behaviour and conformational stability as a function of pH and i.s. have been determined and theoretically interpreted for a variety of salting in/salting out electrolytes and non-polar environments [25, 26].

The supramolecular organization of fibre-forming collagen starts with the occurrence of liquid crystallinity in concentrated solutions. Giraud-Guille [27] reported the formation of cholesteric mesophases *in vitro* above a critical volume fraction $v^*>0.1$, a result consistent [12] with molecularly dispersed triple-helices with the persistence length in table 1. Murthy [28] reported that liquid crystallinity could be detected only in the pH range 2.4–3.0. At larger pH, gelation was accompanied by formation of fibrils that could be oriented in a magnetic field. Crosslinking allowed the stabilization of the oriented gel.

Fibrils, the next hierarchical step in the supramolecular organization of collagen, show significant differences between types I and II, as well as morphological variations upon assembly conditions. The length of the fibril, reflecting the axial arrangement of triple-helices with a stagger equivalent to 1/4.4 (or 67 nm) their molecular length, has been difficult to study but could attain the mm range [29]. Only a short range, liquid-like order is often seen in the direction perpendicular to the fibril axis, and an analogy with smectic liquid crystals has been suggested [30]. Reported diameters vary in the range 10–500 nm, corresponding to different numbers of aggregated molecules, i.e. a 100 nm diameter fibril contains ~4 000 triple-helices [30]. Fertala *et al.* [23] showed that recombinant procollagen II fibrils were thinner (diameter 10–40 nm, possibly with a bimodial distribution [31]), and had a more pronounced arcade-like geometry than collagen I fibrils. Basic vitreous fibrils were also found to be thin and rather uniform in their diameter (14.5 nm) [32].

There is still a controversy regarding the fibrillar packing, growth, and polymorphism of collagen [30, 33]. Hulmes *et al.* elaborated a model in which molecular packing is organized concentrically about the core of the fibril [30]. It is rather important to appreciate that the lateral growth of fibrils is controlled by chemical information encoded in the triple-helices [23], and by surface modification [29]. It might also be programmed for the intended mechanical properties [33].

A more detailed analysis of the different fibrillogenesis of collagen I and II is to be presented elsewhere [34]. Basic collagen fibrils also have the property of assembling into thicker bundles [35]. Early X-ray diffraction data for highly swollen collagen tendons showed that the equatorial spacing between adjacent triple-helices (1.43 nm) is essentially unaltered in spite of a ten-fold increase of the overall and cross-sectional degree of osmotic swelling occurring at pH=2 [26, 36]. This result supports the occurrence of basic fibrillar units resisting swelling and interconnected by swellable and less organized collagenous material. We also observe that the axial ratio (L/d) of an assembling fibril growing more along the longitudinal than lateral direction, increases over the value of the single molecule, see figure 3 (*a*). Therefore, transient liquid crystallinity for a dispersion of thin fibrils may occur at much lover v^* than discussed above for molecularly dispersed triple-helices, becoming an inescapable precursor of the ordering process [34, 37].

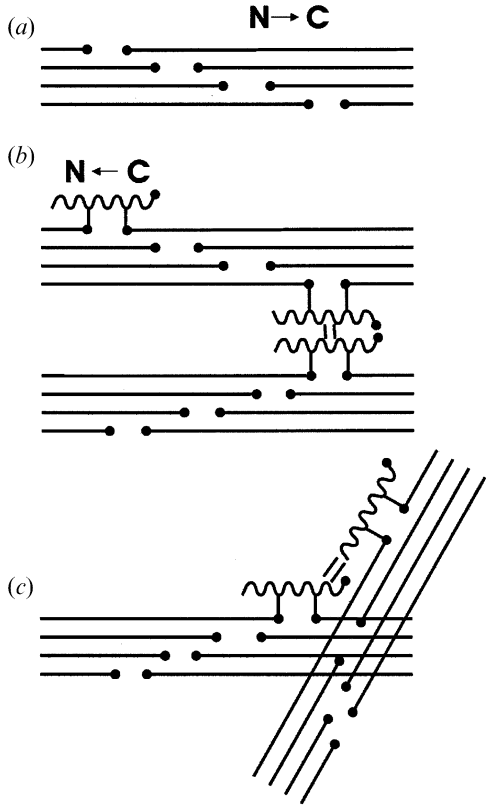

Figure 3. (*a*) Staggered growth of a four-stranded collagen II fibril with L increasing faster than *d*. (*b*) Type IX-type II collagen interactions indicating their antiparallel arrangment and the possibility of linking different fibrils, even (*c*), with different orientation [48].

2.4. *Incompatibility*

In analysing the above results, one is impressed by the prevailing incompatibility of the major constituents. Interaction parameters (χ) estimated from the prevailing non-bonded interactions between atomic groups [38–41] quantitatively show the chemical incompatibility between protein and polysaccharide chains (i.e. collagen/HA, collagen/CS) and even between HA and CS due to the uncharged sulphate groups of the latter. Moreover, the persistence length and the mesophase studies discussed above reveal that collagen develops liquid crystallinity, in contrast to the cases of HA and CS. Thus, the additional possibility of conformational incompatibility [41–43], causing a mesophase separation of HA from a collagen solution at $v > v^*$, should also be considered.

Specific supramolecular interactions between the components might favour their compatibility. However, even at the physiological i.s., the residual polyanion character of HA and particularly CS favours their electrostatic repulsion. Collagen fibrils, already close or below the crystallization boundary, have a tendency to aggregate into large fibrils rather than forming H-bonds with the polysaccharides.

The foregoing considerations appear to contradict the expectation that strong supramolecular bonds stabilize functional supramolecular structures [44]. Moreover, the role of collagen as a reinforcing agent of the gel is perplexing in view of its strong tendency to grow fibrils of larger diameter and to phase-separate. Composite theory prescribes that a fine distribution of the components, down to the molecular level [45], is necessary for heterogeneous reinforcement with optimum blend of properties.

To prevent phase-separation, stabilizing intimate mixtures of incompatible components, polymer engineers have followed several strategies. These include chemical functionalization, crosslinking, interpenetrating networks, and fast mixing followed by quenching below a transition temperature [38]. As discussed in the following section, chemical decoration and supramolecular crosslinking were the strategies followed by Nature for stabilizing the composite structure of the vitreous gel.

3. Assembled components

3.1. *Proteoglycan*

A covalent attachment of chondroitin sulphate side chains to a core protein (e.g. collagen IX) is the main feature of comb(brush)-like proteoglycan structures. The schematization in figure 4 (*a*) includes a globular protein (G1) covalently linked to the *N*-terminal of the core chain. The globular protein can form supramolecular aggregates with HA stabilized by a link protein [46]. Several proteoglycan types occur in various tissues, differences are manifested in the core protein, number, distribution and type of CS side chains [7].

The best characterized molecule appears to be aggrecan [20] showing nanometric-scale resolution by AFM images of the protein core (~300 kD), link protein (~45 kD), GAG number (~100), size (~20 kD), distribution, and composition (C4S vs C6S). Its persistence length, (q~80 nm), affected by age and disease, reveals a large rigidity with respect to the non-assembled components (table 1). Type IX collagen and versican are the prevalent proteoglycans in vitreous gel, respective concentrations being ~2 and ~21 $\mu g\,ml^{-1}$; C6S and C4S prevailing, respectively, in the former and latter proteoglycan [7].

The occurrence of chemical bonding between the core protein and the GAG polysaccharides allows proteoglycans to bypass the incompatibility of the components. The electrostatic repulsion of the charged side chains will prevent close contact among rigid proteoglycan

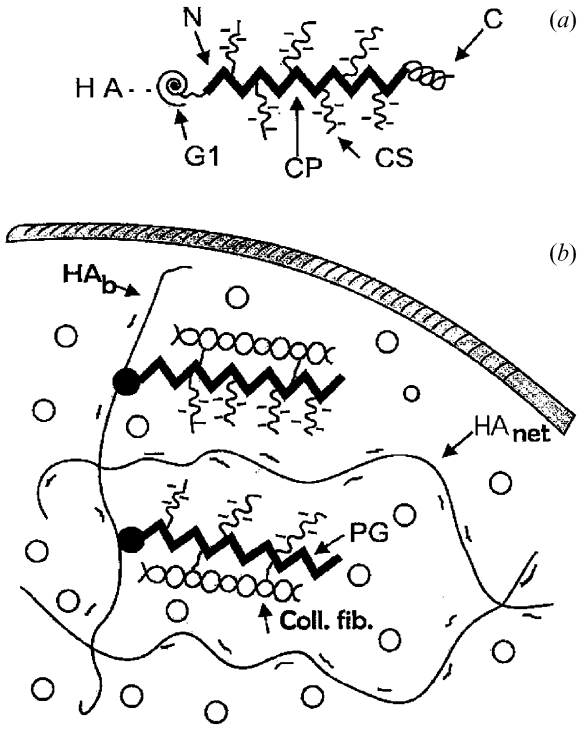

Figure 4. (*a*) Schematization of the basic features of proteoglycans. The core protein (CP) with *C* and *N* terminals has chondroitin sulphate (CS) side chains and a globular domain (G1) at the *N*-terminal, having sites for supramolecular binding to HA. (*b*) Schematization of detailed local organization of major vitreous components. The proteoglycan (PG) is now supramolecularly linked at its G1 site to hyaluroran chains (HA_b). Collagen II fibrils (coll. fib.) and bundles are chemically linked to the proteoglycan in an antiparalled orientation. The functionality at the binding site involving G1, HA and link protein is assumed=2. Unbound HA chains form an entangled network (HA_{net}). Open circles (○) water; minus signs (-) fixed negative charges.

molecules, probably contributing to the compressive modulus of the assembly [47]. Most importantly, the proteoglycans are suitable for the next steps of the assembly of the vitreous structure: decoration of collagen II, and supramolecular linking to HA, as discussed below.

3.2. *Decoration of collagen II fibrils*

The regulation of the fibrillar size is a key issue on the stability of the vitreous gel: we know that collagen fibrils having diameters in the 10 nm range under normal condition may attain macroscopic dimension during liquefaction. Tick collagen II fibrils formed by fused [23] or bundled [35] thinner ones were also detected by electron microscopy. There is a consensus of opinion regarding the stabilization of thin vitreous fibrils by surface 'decoration', although there is no definite agreement on the nature of the coating species [1, 29].

It is relevant to observe that collagen II, collagen IX and GAG chains were observed to form during the early stage of the biosynthesis of the vitreous gel [1]. The formation of HA was instead associated to the postnatal increase of the volume of the vitreous cavity [1]. Therefore, the often suggested decoration of collage II by proteoglycans appears a most plausible mechanism to prevent fusion of collagen II fibrils [48]. Studies performed on bovine cartilage collagen II interacting with collagen IX molecules revealed that the three chains α1(IX), α2(IX), α3(IX) on the COL2 domain each included a site at their *N*-terminal, to which the amino-telopeptide on the α1(II) chain of collagen II might covalently bind [48]. Models for the collagen II-collagen IX interaction, schematized in figures 3 (*b*, *c*) show the antiparallel arrangement of type II fibril and type IX molecules, including head-to-tail association of the latter and the possibility of forming bundles of fibrils, even with different angular orientation. Type II-type IX alignment was also characterized for vitreous collagen [32]. The decorating molecule in the case of cartilage collagen was unlikely to be a proteoglycan since there was no electrophoretic evidence for GAG chains attached to the collagen IX of bovine cartilage.

GAG chains do occur in the vitreous type IX collagen and will further decrease the likelihood of lateral fibril growth due to electrostatic repulsion. Bishop *et al.* reported, however, that depolymerization of CS chains does not alter the short term stability of the gel [1, 49]. Several different molecules and proteins may indeed decorate the fibril surface to prevent formation of thick fibres. Opticin, a member of the small leucine-rich proteoglycan family, binds to the surface of the vitreous fibrils and has a cluster of sialyated *O*-linked oligosaccarides rather than GAG chains [1].

3.3. *Decorated fibrils+HA*

As indicated in the previous section, the synthesis of HA follows the deposition of proteoglycan and collagen fibrils. However, chemical and conformational incompatibility of HA with these assembled components will be even larger than that experienced by the single dispersed components. In particular, the conformational incompatibility will be enhanced by the large persistence length of the proteoglycans (cf. table 1) and the large axial ratio of the collagen fibrils (§ 2.3). An impasse to an efficient dispersion of HA within the proteoglycan–fibril dispersion will result. A mixing dilemma of this type would be solved by a nanotechnologist through the introduction of binding sites allowing a strong specific interaction between the components. We believe that this is indeed the strategic function of

the G1 and link proteins attached to the *N*-terminal of the proteoglycan, see figure 4 (*a*).

The model we envisage requires the first synthesized HA to permeate the proteoglycan–fibril dispersion by recognition of the strong binding sites at the G1-link protein location. A supramolecular connectivity involving high molecular mass HA and the proteoglycan–fibril dispersion will thus be established. Following saturation of the G1-link protein binding sites, self-recognition will allow additional (unbound) HA to permeate the structure forming an entangled network within which the assembly of proteoglycan–fibril-bound HA is interdispersed. A schematization of the postulated local distribution of components is shown in figure 4 (*b*).

The connectivity pattern of the proteoglycan–fibril-bound HA assembly will depend upon the functionality of the binding sites connecting HA with G1 and link protein [44]. A functionality=2, schematized in figure 4 (*b*), allows for a connectivity of the proteoglycan–fibril units as side chains of long HA molecules. Larger functionality would allow a three-dimensional supramolecular network. In the latter case, the gel might include two interpenetrating networks, one stabilized by the supramolecular bonds between HA and the proteoglycan, the other by entanglements and H-bonds between unbound HA molecules. We are unable to find data for assessing the actual functionality of the HA-G1-link protein bond. Indirect evidence deduced from the work of Brewton and Mayne supports a functionality=2 [50]. Alternative models for the local organization of decorated fibrils have been reviewed [1].

Some experimental data are consistent with the postulated occurrence of associated species involving proteoglycan–fibril-bound HA interdispersed within a network of unbound HA. Brenton and Mayne observed by TEM the occurrence of three-dimensional networks of hyaluroran and of HA-binding macromolecules [50]. Gribbon *et al.* reported no evidence of chain association in concentrated solutions of HA in various solvents [17]. Reardon *et al.* confirmed the occurrence of HA aggregating proteoglycans and link protein in mammalian vitreous gel [7]. They concluded that the molar concentration of HA is about 150 times larger than the combined concentration of proteoglycan and link protein (in a 1:1 molar ratio), and therefore the density of the latter along the hyaluroran is much smaller than in the case of more dense tissues. Bishop concluded that while the removal of HA from the vitreous gel (by enzymatic digestion) did not alter the gross, short term distribution of fibrils within the gel, a small percentage of hyaluroran (6%) appeared to be involved in maintaining its finer structure [1, 49].

3.4. *The structured network*

The local organization of major components schematized in figure 4 (*b*) does not account for the regular distribution, shown in figure 1 (*a*), of the fibrillar component within the hyaluronan network. The long range organization of the fibrillar component has been the object of extensive, unresolved debate [1]. The occurrence of a contiguous network of collagen, including bundles of single fibrils with random branches connecting different bundles, was demonstrated by electron microscopy [35, 51]. The size and constitution of the linking filaments were also characterized. The proteoglycan–fibril-bound HA assembly described in the previous section may therefore be associated with a collagen network. The issue is whether the final ordered distribution of fibrils is determined by the collagen network, or whether the latter stabilizes a preexisting distribution encoded in the initial deposition of decorated fibrils. To analyse the origin of the ordered distribution we refer to the case of confinement-induced supramolecular orientation over interacting surfaces. The conceptual analogy is with the orientation of cholesteric liquid crystals confined between parallel glass plates, when the planar (or fingerprint type) orientation achieved by treating or rubbing the anchoring plates, is transmitted to the subsequent layers. It is well know that the orientation can be altered, attaining the perpendicular one, by applying external fields, or increasing the plate spacing [52]. Confinement-induced orientation and morphologies, recently reported for a cylindrical confinement of block copolymers within nanopores, were also related to wall surface–polymer interaction and to pore diameter [53].

As already indicated, the components of the decorated fibrils are formed during the early stage of the biosynthesis, when the volume of the vitreous cavity is small and HA is absent [1, 54]. In the vitreous cortex, figure 1 (*a*), bundles of fibrils are firmly adherent to the retina, and oriented parallel to the retinal surface. For rather small diameters of the vitreous cavity, and in the absence of other components, it is reasonable to assume that confinement-induced orientation will be transmitted to concentric layers confined by the retina. However, as the diameter of the vitreous gel grows due to the postnatal synthesis and diffusion of HA, one expects an alteration of confinement orientation, particularly toward the centre of the gel. Moreover, the swelling due to the permeation of HA will promote an opening up (splay) of the bundles, generating a network of collagen fibrils and residual bundles all over the spherical surface and the interior of the gel. An additional perturbation to a concentric orientation is due to the occurrence of a region, the basal vitreous, cf. figure 1 (*a*), in which fibrils

are oriented normal to the retina. The actual distribution of fibrils in figure 1 (*a*) appears qualitatively consistent with the above sequence of events. This complex, extremely efficient reinforcement scheme of the vitreous gel might be simulated in terms of gel growth, splay of the bundles due to HA permeation, and the competing planar and perpendicular orientations at different sites on the retinal surface.

Support for the postulated effect of swelling by HA on the spreading of fibrils over the gel volume comes from the work of Puett *et al.* [36] discussed in § 2.3. Bishop *et al.* [1, 49] reported that removal of collagen fibrils by collagenase digestion caused a complete gel collapse, whereas digestion of up to 94% HA did not alter the vitreous structure. These critical tests are not inconsistent with the model outlined above. In fact, the small fraction of bound HA, which assures the connectivity of decorated fibrils, has a built-in memory of the *final* (adult) gel structure, preventing its collapse upon removal of unbound HA. This built-in memory is related to the supramolecular nature of the connectivity at the G1-HA_b interaction sites. A covalent connection would have assured a memory of the structure occurring at the initial stage of gel formation: removal of unbound HA subsequenty admitted to that structure would have resulted in gel collapse to that initial stage. Supramolecular bonds undergo instead dynamic rearrangement allowing a release of strain on the connecting chains during growth; also note in figure 3 (*c*) the possibility of tethering fibrils at variable orientation. This property was highlighted in recent studies on supramolecular networks [44, 55] and in early work on networks having labile crosslinkages [56].

3.5. *Liquefaction*

The prevailing opinion is that liquefaction is promoted by changes in non-collagenous components acting as surface coatings and spacers for the collagen fibrils. Further aggregation of collagen fibrils thus occurs (to a size visible by light microscopy) producing a denser gel, its detachment, and collagen-free liquefied areas.

It is important to appreciate that the same concentration of hyaluronan was detected in the gel and in the sol [57]. The theory of network swelling in open thermodynamic systems requires equal activities in the sol and in the gel for all components free to migrate across the equilibrium boundary [58]. The equal concentration of HA in both phases can therefore be assumed to confirm that unbound HA is not participating in a crosslinked network. Unbound HA should indeed be regarded as a swelling agent for the proteoglycan–fibril-bound HA assembly. The same theory suggests that deswelling will be produced by: (i) an increase of the connectivity or degree of crosslinking of the gel, and (ii) a reduction of fixed charges within the gel domain. Negative charges occur on both CS and HA. However, we have seen that HA (unbound) is not anchored to gel structure. Moreover, the experiments by Bishop *et al.* already cited reveal that CS can be depolymerized without short term alteration of the gel structure. Therefore, the electrostatic repulsion between the polyanions may contribute to, but does not control, the stability of the gel. Thus, the shrinkage occurring during liquefaction is necessarily associated with an increase of the connectivity of the components.

Our approach cannot, however, suggest the corresponding chemical alterations during aging. Bishop *et al.* suggested an age-induced loss of collagen IX resulting in a decreased decoration and fusion of collagen II fibrils [51]. The age-induced alteration of chondroitin sulphate side chains might have an influence on the long term stability of the gel [49]. The complexity of the alterations is, however, demonstrated by a recent LM and TEM study by Los *et al.* of the transitional area between gel and liquid [59]. The main event they observed was not fibrillar aggregation, but rather a fragmentation of fibrils. They observed changes in the distribution of both fibrils and proteoglycans. In the normal vitreous gel they report near-regularly spaced proteoglycans oriented at various angles to collagen II fibrils in a quasi-parallel orientation. In the transition zone, proteoglycans lost their orderly distribution and aggregated along the collagen fragments. They suggested that fibril association might not control liquefaction. Moreover, they suggested that an extracellular enzymatic degradation of fibrillar collagen and proteoglycans, as well as collagen turnover (synthesis and degradation), ought to be considered.

4. Conclusions

We have compared literature data with expectations based on chemical/conformational compatibility, mesophase and other supramolecular interactions among the major components of the vitreous gel. The sequence of assembling steps consistent with both experiments and theoretical expectations includes the following features. The connectivity framework needed for the stabilization of the gel is based on the supramolecular association of a minor fraction of the total HA with proteoglycan-decorated collagen fibrils. The decoration allows the formation of fibril bundles but not the fusion into thicker fibrils. The framework, established at the early stage of growth, is subsequently swollen by a larger fraction of unbound HA. The distribution of collagen fibrils within the mature gel results from an ordering

process in confined regions, evolving into a network connectivity through a splay-type deformation of fibrillar bundles. Liquefaction reflects an increased connectivity consistent with the swelling theory for open systems. However, the detailed chemical transformations during liquefaction cannot be assessed by the present approach. A deeper knowledge of the vitreous biomolecular structure will allow the development of functional surgical substitutes and improve pharmacokinetic characteristics of drugs for intravitreal use.

Acknowledgments

We express our great appreciation to Prof. P. N. Bishop for reading the draft and for constructive comments; also to Mrs Cinzia Bongianni and Dr Luciano Galantini for essential contributions to the assembly of the manuscript.

References

[1] P.N. Bishop. *Prog Retina Eye Res.*, **19**, 323 (2000).
[2] R.L. Zimmerman. *Biophys. J.*, **29**, 539 (1980).
[3] J. Sebag, E.A. Balazs. *Invest. Ophthalmol. Vis. Sci.*, **30**, 1871 (1989).
[4] J. Grimshaw, A. Kane, J. Trocha-Grimshaw, A. Douglas, U. Chakravarthy, D. Archer. *Electrophoresis*, **15**, 936 (1994).
[5] E.A. Balazs, J.L. Denlinger. In *Aging and Human Visual Function*, N. Dismukes, R. Sekular (Eds), pp. 45–57, Alan R. Liss, New York (1982).
[6] R. Mendichi, L. Soltés, A. Giacomatti-Schieroni. *Biomacromolecules*, **4**, 1805 (2003).
[7] A. Reardon, D. Heinegard, D. Mclead, J.K. Sheehan, P.N. Bishop. *Matrix Biol.*, **17**, 325 (1998).
[8] A. Almond, A. Brass, J.K. Sheehan. *J. mol. Biol.*, **284**, 1425 (1998).
[9] J.E. Scott, F. Heatley. *Biomacromolecules*, **3**, 547 (2002).
[10] M. Bathe, G.C. Ruthedge, A.J. Grodzinsky, B. Tdor. *Biophys J.*, **88**, 3870 (2005).
[11] A. Ciferri. In *Liquid Crystallinity in Polymers*, A. Ciferri (Ed.), pp. 209–259, V.C.H., New York (1991).
[12] P.J. Flory. *Statistical Mechanics of Chain Molecules*, Wiley, New York (1969).
[13] T. Odijk. *J. polym. Sci. polym. Phys.*, **15**, 477 (1977).
[14] D.A. Gibbs, E.W. Merrill, K.A. Smith. *Biopolymers*, **6**, 777 (1968).
[15] E. Fuissac, M. Milas, M. Rinaudo. *Macromolecules*, **26**, 6945 (1993).
[16] P. Gribbon, B.C. Heng, T.E. Hardingham. *Biophys. J.*, **77**, 2210 (1999).
[17] P. Gribbon, B.C. Heng, T.E. Hardingham. *Biochem. J.*, **350**, 329 (2000).
[18] R.H. Pearce, B.J. Grimmer. *Biochem. J.*, **157**, 753 (1976).
[19] A.J. Deutsch, R.J. Midura, A.K. Plaas. *J. Orthop. Res.*, **13**, 230 (1995).
[20] L. Ng, A.J. Grodzinsky, P. Patwari, J. Sandy, A.K. Plaas, C. Ortiz. *Struct. Biol.*, **143**, 242 (2003).
[21] M.T. Bayliss, D. Osborne, A. Woodhouse, C. Davidson. *J. biol. Chem.*, **274**, 15892 (1999).
[22] H. Boedtker, P. Doly. *J. Am. chem. Soc.*, **78**, 4267 (1956).
[23] A. Fertala, A.L. Sieron, Y. Hojima, A. Ganguly, D.J. Prockop. *J. biol. Chem.*, **269**, 11584 (1994).
[24] Y.L. Sun. *J. Biomechanics*, **37**, 1665 (2004).
[25] E. Bianchi, A. Ciferri, G. Conio, D. Puett, L.V. Rajagh. *J. biol. Chem.*, **242**, 1361 (1967).
[26] A. Ciferri. In *Treatise on Skin*, Vol. 1, H.R. Elden (Ed.), pp. 103–146, Interscience, New York (1971).
[27] M.M. Giraud-Guille. *J. mol. Biol.*, **224**, 861 (1992).
[28] N.S. Murthy. *Biopolymers*, **23**, 1261 (1984).
[29] T.J. Wess. *Adv. protein Chem.*, **70**, 341 (2005).
[30] D.S. Hulmes, T.J. Wess, D.J. Prockop, P. Fratzi. *Biophys. J.*, **68**, 1661 (1995).
[31] J.E. Saunders. *J. Biomech*, **34**, 1581 (2001).
[32] K.J. Bos, D.F. Holmes, K.E. Kadler, D. McLeod, N.P. Morris, P.N. Bishop. *J. mol. Biol.*, **306**, 1011 (2001).
[33] V. Ottani, D. Martini, M. Franchi, A. Ruggeri, M. Rasponti. *Micron*, **33**, 587 (2002).
[34] A. Ciferri, On Collagen II Tibrillogenisis (submitted).
[35] K.J. Bos, D.F. Holmes, R.S. Meadows, K.E. Kadler, D. McLeod, P.N. Bishop. *Micron*, **32**, 301 (2001).
[36] D. Puett, A. Ciferri, L.V. Rajagh. *Biopolymers*, **3**, 439 (1965).
[37] A. Ciferri, W.R. Krigbaum. *Gazz. Chim. Italiana*, **116**, 529 (1986).
[38] F.H. Case, J.D. Honeycutt. *Trends polym. Sci.*, **2**, 259 (1994).
[39] D.R. Paul, S. Newman. *Polymer Blends*, Academic Press, New York (1978).
[40] D.R. Paul, J.W. Barlow. *Polymer*, **25**, 487 (1984).
[41] E. Bianchi, A. Ciferri, G. Conio, E. Marsano, A. Tealdi. *Macromolecules*, **17**, 1526 (1984).
[42] P.J. Flory. *Adv. polym. Sci.*, **59**, 1 (1984).
[43] A. Ciferri. *Liq. Cryst.*, **33**, 555 (2006).
[44] A. Ciferri. In *Supramolecular Polymers*, 2nd Edn, A. Ciferri (Ed.), pp. 29–75, CRC Press, Boca Raton (2005).
[45] A. Ciferri. *Polym. Eng. Sci.*, **34**, 377 (1994).
[46] F. Binette, J. Cravens, B. Kahossi, D.R. Haudenshild, P.F. Goetinick. *J. biol. Chem.*, **269**, 19116 (1994).
[47] M.D. Bushman, A.J. Grodzinsky. *J. biomech. Eng.*, **117**, 179 (1995).
[48] J-J. Wu, P.E. Woods, D.R. Eyre. *J. biol. Chem.*, **267**, 23007 (1992).
[49] P.N. Bishop, P. McLeod, A. Reardon. *Invest. Ophthamol. Vis. Sci.*, **40**, 2173 (1999).
[50] R.G. Brewton, R. Mayne. *Exp. Cell. Res.*, **198**, 237 (1992).
[51] P.N. Bishop, D.F. Holmes, K.E. Kadler, D. McLeod, K.J. Bos. *Invest. Ophtamol. Vis. Sci.*, **45**, 1041 (2004).
[52] M. Kleman. In *Liquid Crystallinity in Polymers*, A. Ciferri (Ed.), pp. 365–394, V.C.H., New York (1991).
[53] B. Yu, P. Sun, D.D. Jin, B. Li. *Phys. Rev. Lett.*, **96**, 138306(1–4) (2006).
[54] E.A. Balazs. *Int. Ophthamol. Clin.*, **15**, 53 (1975).
[55] R.P. Sijbesma, F.H. Beijer, L. Brunsveld, B.J.B. Folmer, J.H.K.K. Hirshberg, R.F.M. Lange, J.K.L. Lowe, E.W. Meijer. *Science*, **278**, 1601 (1997).
[56] R.D. Andrews, A.V. Tobolsky, E.E. Hanson. *J. appl. Phys.*, **17**, 352 (1946).
[57] L. Larsson, S. Osterlin. *Graefe's Arch. clin. exp. Ophthalmol.*, **223**, 92 (1985).
[58] D. Volpin, F. Mistrali, G.B. Garibaldo, A. Ciferri. *J. phys. Chem.*, **75**, 142 (1971).
[59] L.I. Los, R.J. van der Worp, M.J.A. van Luyn, J.M.M. Hooymans. *Invest. Ophtamol Vis. Sci.*, **44**, 2828 (2003).